

# In-depth analysis of the current state of knowledge on lead-telluride glasses and their properties

Rajiv Pandey<sup>1\*</sup>, A. K. Sharma<sup>2</sup>, Ghizal. F. Ansari<sup>3</sup>

<sup>1,2,3</sup> Department of Physics, Madhyanchal Professional University, Ratibad, Bhopal, India

<sup>1</sup> E-Mail: rajeev9939160108@gmail.com

**Abstract** - Significant amounts of research on glasses have been focused on complicated glasses like tellurite and phosphotellurite as their principal research topics since the 1960s and 1970s. As is the case with glasses containing tellurium dioxide, well-known glasses also incorporate additional cations as matrix modifiers, as is also the case with glasses containing tellurium dioxide. Numerous researchers have investigated the spectroscopic properties of rare earth ions found in tellurite glasses. The investigation by comparing and contrasting the optical spectra of  $Pr^{3+}$ ,  $Nd^{3+}$ ,  $Eu^{3+}$ ,  $Ho^{3+}$ , and  $Er^{3+}$  in  $Na_2O$ - $TeO_2$  glasses with those of the same species in silicate and fluoroberyllate glasses. After making the discoveries that the activator-ligand interaction in tellurite is more covalent than the interaction in fluoroberyllate glass, that tellurite's site symmetry is lower than that of fluoroberyllate glass, and that tellurite's average crystal field at the rare earth site is lower than that of silicate glasses, they came to the conclusion that tellurite is the more advantageous material. The literature review of this study was carried out by screening various global data sets including the web of science, Scopus, PubMed, NIH library and Science Direct. The main aim of this study was to assemble and categorize the synthetic and characteristic properties of lead based telluride glasses.

**Keywords** - Glasses, Lead telluride glasses, Melt-quenching, Spectroscopy, X-Ray Diffraction

-----X-----

## INTRODUCTION

Tellurite glasses are utilised in a variety of subfields of scientific research, and due to the beneficial properties that they possess, such as their high refractive index, high polarizability, and strong non-linear third order optical susceptibility. Tellurite glasses are utilised in a variety of subfields of scientific research due to the beneficial properties that they possess. Waveguides and other types of optoelectronic devices are able to produce low-loss, ultrafast optical transmission with the help of these glasses. [1-7]

Research conducted using neutron diffraction demonstrated that the network that constitutes  $TeO_2$  glass is made up of  $TeO_4$  trigonal bipyramidal (tbp) and  $TeO_3$  trigonal pyramidal units. In addition, between 68 and 74% of the Te ions are coordinated in tetrahedral frameworks. When alkali, alkaline-earth, heavy metal, transition, and rare-earth ions are added to glasses, a change takes place in the tellurite network, and the Te-O coordination number decreases. The glass-forming ability (GFA) of the tellurite material is directly impacted by the quantity of metal oxides that are present in the tellurite material. Numerous scientific articles have been devoted to the examination of the structure of tellurite glass. [8-14]

Glasses, as opposed to crystals, have a structure that is disorganised, which makes them materials that are isotropic and often do not show birefringence. Crystals, on the other hand, have a structure that is organised. Glasses lose their isotropy and turn into materials with optical birefringence when they are subjected to stresses caused by mechanical fields, magnetic fields, or electric fields. This suggests that the change in the refractive index takes place not just in the direction of the applied stress but also in the direction that is normal to it. Although Brewster was the first person to detect photo-elasticity, it is possible that Mueller's theory might provide some light on why this phenomena occurs in non-crystalline materials like glasses. This would be the case if Mueller's theory were correct. If Mueller's theory had any potential to shed any light on the situation, then this would be the case. It has been shown that stress-induced birefringence may be traced back to atomic deformation as well as the Lorentz-Lorentz interaction that occurs in the material. This is something that can be done. This optical phenomena that is brought on by stress has been investigated in great depth using a broad range of various kinds of materials. Short-range structural characteristics, such as the ratio of the cation (metal

ion)-oxygen bond length ( $d$ ) and the cation coordination number ( $N_c$ ), are used in the modelling of the stress-optic or photoelastic response. The optical stresses of binary compositions of heavy metal oxide tellurite glasses may be either positive, negative, or zero. Binary compositions of heavy metal oxide tellurite glasses may take a few different forms, two of which are  $PbO-TeO_2$  and  $BaO-TeO_2$ . [15-20]

In this review article we summarize the latest synthetic, characteristic and property features of lead based telluride glasses.

### Lead telluride glasses

Sayyed and colleagues synthesised glass-ceramics in 2021 by subjecting them to regulated heating and cooling, resulting in the formation of a formula that read  $(39.5-x)$ . The XRD analysis shows that the crystalline phases of the network are made up of 40%  $PbO$ , 20%  $B_2O_3$ , 20%  $TeO_2$ , 20%  $MgO$ , 0.5 mol%  $Dy_2O_3$ , and  $x$  mol%  $Tb_2O_3$  (where  $x$  may be any of the following values: 0%, 0.5 mol%, 1, 1.5, 2, and 2.5 mol%). Through the use of FTIR to quantify vibrational velocities, network structural bonds were identified and characterised. The band gaps for direct transitions decrease from 3.209 to 3.025 eV while the band gaps for indirect transitions decrease from 3.006 to 2.637 eV when there is a rise in the concentration of terbium. In order to evaluate the capacity of the materials to obstruct gamma rays, the MCNP5 approach was used. The linear attenuation coefficients (LAC) that were calculated by MCNP5 and confirmed by XCOM are different from one another by a margin of less than 6%. At lower energies (0.347 and 0.662 MeV), the addition of  $Tb_2O_3$  had an effect on the LAC values, and this effect resulted in a considerable decrease when a greater quantity of  $Tb_2O_3$  was added to the glasses. This was possible as a result of  $Tb_2O_3$ 's ability to lower LAC. Sayyed et al. used the simulated LAC to calculate the half-value layer for the TNNS0-TNNS2.5 glasses (HVL). In every single one of the TNNS0.0-TNNS2.5 glasses, there was a correlation between HVL and power that was in the positive. The half-width at half-energy (HVL) increased from 0.37 centimetres at 0.284 MeV to 0.99 centimetres at 0.5 MeV, 1.62 centimetres at 0.8 MeV, and 2.3 centimetres at 1.332 MeV for TNNS0.5. The HVL researchers found that these glasses needed to be significantly thinner in order for them to be effective in absorbing low-energy radiation. This was one of their discoveries. When they were employed in the past to absorb high-energy radiation, these glasses did not have this characteristic at all. Calculations were done to determine the HVL of TNNS0.0 glasses and then compared to the HVL of TNNS0.5 glasses. In addition, the TNNS0.0/TNNS2.5 HVL ratio was calculated with the purpose of gaining a deeper comprehension of the influence that the glass composition has on the HVL results. Because every ratio was more than 1, it is abundantly evident that TNNS0.0 has a larger HVL than the other case. [21]

The glass formation and thermoelectric characteristics of lead telluride ( $PbTe$ ) amorphous alloys were explored by Li et al., 2021. There is reason to be optimistic about the potential of a revolutionary process known as vitrification to boost the thermoelectric performance of lead telluride-based materials ( $PbTe$ ). In order to accomplish this objective, complicated and disordered structures are created, which has the effect of making the lattice less heat conductive. In spite of the fact that vitrifying  $PbTe$ -based alloys might be a challenging process, it is still necessary to have a comprehensive understanding of the glass-making process. Both thermodynamic and kinetic parameters are taken into consideration in this research on the production of glass from  $PbTe$  alloys. Low entropy of fusion ( $S_m$ ) and a deep eutectic way were found to be the two most important aspects in the glass-forming potential of  $(PbTe)_x(Ga_2Te_3)_{100-x}$  and  $(PbTe)_x(In_2Te_3)_{100-x}$  alloys, respectively. The composition range of  $x = 52-64$  was found to be an accurate description of the glass-forming zone in freshly formed  $(PbTe)_x(Ga_2Te_3)_{100-x}$  glasses. This was established by conducting experiments. The ideal component for glass should have a thermal conductivity of 0.1  $Wm^{-1}K^{-1}$  when measured at 300 K (the formula for this value is  $(PbTe)_{61}(Ga_2Te_3)_{39}$ ). [22]

The fact that Sathish and his associates (2015) In order to make the standard glasses, first the components were melted together, and then the molten liquid that was created was heated for thirty minutes at a temperature of 280 degrees Celsius ( $x = 0.1$  mol% and 0.2 mol%). The SEM examination revealed that the samples were composed of glass ceramics. When impurities are present, the values for glass ceramic XRD properties such as crystallite size drop to 184-109Å°. The number of micro stresses and dislocations in the material is increasing at an alarming rate. DSC data show that both the temperature at which the glass transition occurs and the thermal stability rise as the amount of impurities in the material increases. The infrared absorption spectra of  $Nb_2O_5$ -doped glasses and ceramics were analysed in order to determine their properties. The vibrating and stretching of  $Te-O$  causes the recording of bands in the resulting sound. In rare earths-doped glass-ceramics, the absorption edge moves to higher energy levels, as can be seen in the optical absorption spectra of  $TeO_2-PbO-Nb_2O_5$ . The concentration of critical glass components followed by their rearranging was the cause of the edge shift that was observed. The absorption spectra of rare earth oxide-doped  $TeO_2$  glasses are consistent with the absorption spectra of other rare earth oxide-doped glasses. [23]

$PbTe$  quantum dots implanted in fluorogermante glass were the focus of the investigation conducted by El-Rabaie et al (2015).  $PbTe$  quantum dots that have been artificially produced have a shift to the blue in their optical absorbance, which is evidence of significant quantum confinement. Nanoparticles with sizes of 3.2 nm, 3.6 nm, 6.1 nm, and 7.3 nm are

produced when glass samples are heated to a temperature of 500 degrees Celsius for 30, 60, 120, and 180 minutes, respectively. The Eopt value decreased from 2.52 to 1.95 eV as a result of increases in the nanoparticle size. Research using X-ray diffraction has shown the presence of cubic PbTe nanocrystals. A comparison of the XRD pattern and the TEM micrograph to the optical absorption spectra is used to validate the quantum dot size. [24]

Research published in 2020 by ChutumunKratatong and his colleagues: Spraying and pyrolyzing thin films of lead telluride on borosilicate and fluorine-doped tin oxide (FTO) glass substrates allowed for the production of both Sb-doped PbTe and undoped PbTe. In support with the ocular observations, the results of the X-ray diffraction (XRD) patterns analysis revealed that the PbTe and PbTe:Sb crystal structures on both substrates had a cubic form. This was determined by analysing the patterns. The optical band gap is increased and the lattice constant is decreased when Sb is introduced into the PbTe lattice structure. The energies of E<sub>g</sub> onset and E<sub>g</sub> end were always in the range of 1.17–1.22 eV and 1.40–1.53 eV, respectively. The introduction of Sb atoms into neighbouring vacancy sites occupied by Pb and Te results in defects and a disturbance of the lattice structure. [25]

The tried and tested technique of melt quenching, which has been used for a long time, was used by Sathish et al. (2011) in order to effectively construct niobium-lead-telluride glass ceramics with the following compositions. This approach has been used for a long time. This material has been assigned the formula  $x\text{Nb}_2\text{O}_5-(20x)\text{PbO}80\text{TeO}_2$  by the chemistry (where x is a weight percentage between 0.1 and 0.5). Samples of amorphous glass were able to crystallise satisfactorily after being subjected to the annealing process at a temperature of 400 degrees Celsius. It was only via the use of X-ray diffraction and scanning electron microscopy that it was eventually brought under control and contained. According to the results of the Debye-Scherrer formula, the particle size distribution of these glass ceramics spans a range that is anywhere from 15 to 60 nanometers. The research that was carried out using a scanning electron microscope (SEM) indicated that the samples at issue include needle-like crystals of some kind. [26]

Research has been carried out in order to get a better understanding of the physicochemical and optical characteristics of glasses that include lead telluride (Pb:TZBN) (Riyatun et al., 2016). A rundown of the many chemical components that go into the production of these glasses is as follows: This substance may have any value between 1.0 and 2.5 mol% for the variable x, which is denoted by the chemical formula  $55\text{TeO}_2-(41-x)\text{ZnO}-2\text{Bi}_2\text{O}_3-2\text{Na}_2\text{O}-x\text{PbO}$ . This is the formula for the compound. The refractive indices, densities, and UV-VIS-NIR spectra of the glasses were all measured while they were allowed to remain at room temperature. At a wavelength of 746 nm, the measurements were made. By using the tauc fitting approach, we were able to determine the energy of the

optical bandgap (E<sub>g</sub>). According to the results of our inquiry, a rise in the concentration of Pb<sup>2+</sup> causes both the refractive indices and the optical bandgaps of the materials to become more noticeable. This is the case even if the quantity of Pb<sup>2+</sup> remains the same. In spite of the fact that the concentration of Pb<sup>2+</sup> has not changed, this is still the case. During the course of our investigation, we looked for a link between the concentration of Pb<sup>2+</sup> and alterations in the electronic polarizability (O<sub>2</sub><sup>-</sup>) or optical basicity. However, we did not discover any such association. [27]

According to Saheb et al., researchers investigated the effect that the thickness of the sample and the lead concentration had on the electrical switching behaviour of Ge<sub>20</sub>Te<sub>80-x</sub>Pb<sub>x</sub>(2x8) glass. In order to stop the glass from melting during the process of making the samples, a quenching furnace was used. Something that seems to be a threshold flipping could be detected in the samples. It has been shown that there is a negative correlation between the amount of lead present and the switching voltages. When the composition is x=5, they exhibit strange behaviour, and when the composition is x=7.4, they are at their most vulnerable. The results of the study indicated that the samples had the ability to withstand a total of 28 switching cycles before latching onto the ON state in a permanent manner. [28]

Bomfim et al. (2008) were the first researchers to characterise the influence of the concentration of Yb<sup>3+</sup> on the frequency upconversion (UPC) of Er<sup>3+</sup> in PbO-GeO<sub>2</sub>-Ga<sub>2</sub>O<sub>3</sub> glasses, to the best of our knowledge. When making the samples, various percentages of Yb<sub>2</sub>O<sub>3</sub> (ranging from 0.5 to 5.0 weight%) and Er<sub>2</sub>O<sub>3</sub> (ranging from 0.5 to 1.0 weight%) were utilised. In reaction to a diode laser with a wavelength of 980 nm, the material produces light with wavelengths of green (523 and 545 nm) and red (657 nm). Excitation power, as well as the frequency of the UPC emission intensity, are both subjects of the analyses that are carried out. Because of this one-of-a-kind property of these glasses, the ratio of red to green emission is increased. This is accomplished by increasing the concentration of Yb<sup>3+</sup>, which is the direct result of an effective energy transfer from Yb<sup>3+</sup> to Er<sup>3+</sup>. In order to do this, this increases the ratio of red emission to green emission. This occurs because to the chance that Yb<sup>3+</sup> will get energy from the glasses, which will then cause it to change into Er<sup>3+</sup>. [29]

(Wang et al., 2004) It has been said that Yb<sup>3+</sup>-doped glasses may be made by combining the elements (mol%) 5La<sub>2</sub>O<sub>3</sub>-2.5K<sub>2</sub>O-2.5Na<sub>2</sub>O with the elements (mol%) 70TeO<sub>2</sub>-(20 x) ZnO-xPbO in the right quantities. This, according to the study, would result in the production of Yb<sup>3+</sup>-doped glasses. We have looked at the thermal stability of Yb<sup>3+</sup> ions as well as their spectra, in addition to doing research on the laser properties of these ions. It was discovered that the glass with the formula 70TeO<sub>2</sub>-15PbO-5ZnO-5La<sub>2</sub>O<sub>3</sub>-2.5K<sub>2</sub>O-2.5Na<sub>2</sub>O has exceptional

stability ( $(T_x T_g) > 190$  degrees Celsius). It measured  $1.25 \text{ pm}^2$  for its stimulated emission cross-section,  $0.94 \text{ ms}$  for its measured fluorescence lifetime, and  $72 \text{ nm}$  for its fluorescence effective linewidth. In addition to that, the glass had an extensive fluorescence effective line. Everything that was discovered at this location came to light as a result of pure and absolute luck. This system glass is ideal for producing short pulses in diode-pumped lasers, high-peak power and high-average power lasers, short pulse generation in tunable lasers, and high-peak power and high-average power lasers. When it comes to the positive potential laser qualities, this system glass is also ideal for producing short pulses in tunable lasers. [30]

Waleed Al Mohammedi, in collaboration with his contemporaries, 2022: The authors of this study believe that readers will be able to get a better knowledge of these more intricate glasses by examining the structure of  $\text{PbI}_2\text{-Ag}_2\text{O-TeO}_2$  glasses. This will be accomplished by researching the structure of these glasses. In order to explore the local environment of Te atoms as well as the crystallisation behaviour of glasses, spectroscopic methods such as Raman vibrational, X-ray diffraction (XRD), and electron diffraction pattern analysis were used (EDP). The method of analysis known as X-ray diffraction (XRD) demonstrates that binary  $\text{Ag}_2\text{O-TeO}_2$  glasses may generate a number of distinct crystalline phases. Despite the fact that  $\text{Ag}_2\text{Te}_2\text{O}_5$  has a more crystalline structure than  $\text{Ag}_2\text{Te}_4\text{O}_9$ , both of these compounds have metastable crystal structures.  $\text{Ag}_2\text{Te}_2\text{O}_5$  is more crystalline. The hypothesis that glasses that have been supplemented with  $\text{Ag}_2\text{O}$  will, at some point in the future, crystallise into clusters of different species is given credence by the high degree of agreement between the results obtained using a transmission electron microscope, an electron diffraction pattern, and an X-ray diffraction experiment (XRD). It is possible to differentiate glasses made using the trenay technique and containing lead iodide from other types of glasses due to the amorphous structure that these glasses possess. It is feasible to categorise structural telluride units according to their unique properties if the Raman spectra of these units are analysed at a high resolution. There are a large number of structural telluride units.  $\text{TeO}_4$  and  $\text{TeO}_3+1$  are the two essential building components that are employed in the process of creating telluride structures. This is because both of these components are telluride oxidation states. On the other hand, anytime the concentration of  $\text{PbI}_2$  is elevated, the creation of  $\text{TeO}_3^-$ ,  $\text{TeO}_3^{2-}$ , and  $\text{Ag-Te}$  species takes place. These species are formed as a result of the reaction. [31]

In the process of producing innovative materials for electrical applications, monodisperse lead telluride ( $\text{PbTe}$ ) nanocrystals with diameters ranging from  $4$  to  $10 \text{ nm}$  serve as the building blocks for quantum dots, as stated by Urban et al. Throughout the whole of this process, the nanocrystals are used in some capacity. Because of the development of two more synthetic processes, it is now feasible to produce nanocrystals

in quantities of up to ten kilogrammes of a single size in vast numbers, or to make nanocrystals of a range of sizes in minute quantities. Methods such as transmission electron microscopy (TEM), X-ray diffraction (XRD), and optical absorption are used in the process of characterising  $\text{PbTe}$  nanocrystals. Neither of these victories could have been won in the past due to insurmountable obstacles.  $\text{PbTe}$  nanocrystal assembly is a process that aims to manufacture nanocrystals with either a short-range (glassy solids) or long-range (superlattices) packing order by altering the conditions under which the crystals are formed. This can result in the formation of nanocrystals with either a short-range (glassy solids) or long-range (superlattices) packing order. The nanocrystals will then be able to be arranged into superlattices as a result of this. High-resolution scanning electron microscopy and grazing-incidence small-angle X-ray scattering (GISAXS) are two techniques that are required for conducting an analysis of the film order and estimating the typical interparticle spacing. Both of these techniques are necessary for conducting an analysis of the film order (HRSEM). Chemical activation has the potential to increase the conductivity of these coatings by  $9\text{--}10$  orders of magnitude, which is a significant possibility. This is based on the assumption that the structure of the quantum dots is preserved. These findings are the product of the very first optical and electrical investigation of  $\text{PbTe}$  solids that has ever been carried out. [32]

The researchers that participated in the study that Silva et al. An examination of the structural makeup of binary tellurite-based glasses in the  $\text{TeO}_2\text{-PbO}$  system was carried out by using spectroscopic techniques such as Raman scattering and X-ray absorption, among others. Both types of spectroscopies demonstrate that there are considerable shifts occurring in the initial coordination shell that surrounds the tellurium atoms as the quantity of  $\text{PbO}$  that is present rises. This reveals lead's activity as a modulator of glassy networks. However, the presence of a medium-range order contribution demonstrates that lead atoms also contribute to the formation of glassy networks. The results of tests using  $\text{Pb L}_3$ -edge EXAFS show that lead atoms fulfil this structural function; however, the existence of this contribution demonstrates that lead atoms also fulfil this structural function. [33]

### Lead telluride glasses doped with neodymium

Absorption by rare-earth  $\text{Nd}^{3+}$  ions takes place at a wavelength of around  $800 \text{ nm}$  (Richards and Jha, 2017) [34], which is in the same range as that of  $\text{Ti:sapphire}$  lasers and laser diodes that are available for purchase commercially. As a consequence of this, these lasers are often used in the process of pumping  $\text{Nd}$ -doped gain medium, such as amplifiers based on tellurite-glass.  $\text{Nd}^{3+}$  ions may be stimulated to the ( ${}^4\text{F}_{5/2}$ ,  ${}^2\text{H}_{9/2}$ ) states by applying a pumping field with a wavelength that is close to  $800 \text{ nm}$ . As a

result of non-radiative multiphonon decay, the shift from the transient ( $^4F_{5/2}, ^2H_{9/2}$ ) states to the higher laser level  $4F_{3/2}$  happens very quickly. Because of the  $^4F_{3/2} \rightarrow ^4I_{11/2}$  transition, it is also possible to see the  $Nd^{3+}$  emission band, which has its maximum at around 1060 nm. Figure 1 presents the  $Nd^{3+}$  energy levels in a format that is more condensed.

It is important to keep in mind that  $Nd^{3+}$  ions may also be pumped by employing wavelengths that are shorter. An  $Nd$ -doped sample that was driven by an Argon laser at 514.5 nm was used to demonstrate the world's first tellurite bulk glass-based laser in 1978 (Michel et al., 1978) [35]. The laser operated at around 1060 nm. Because of the development of Ti:sapphire lasers and laser diodes, it is no longer required to use secondary pump sources for  $Nd$ -doped gain elements.

**Laser Amplification Using  $Nd$ -Doped Fibers:** In the scientific literature, tellurite glass fibre lasers were initially mentioned for the first time in 1994 (Wang et al., 1994) [36]. a length of fibre measuring 0.6 metres that is composed of  $76.9TeO_2-15.5ZnO-6.0Na_2O-1.5Bi_2O_3-0.1Nd_2O_3/75TeO_2-20ZnO-5Na_2O$  glass core/cladding composite was pumped by a Ti:sapphire laser operating at 818 nanometers. Instead of using external mirrors to set up the resonator, Fresnel reflection with a coefficient of 11.9% was employed from each fibre end. The core of the fibre has the form of an oval throughout its whole. The slope efficiency of the power output at one end of the fibre was determined to be 23% in relation to the power that was input by the pump. If we make the assumption that both ends of the slope create the same amount of emission, then we should be able to determine that its efficiency is 46% higher than the threshold. Approximately 27 milliwatts was where the shutdown occurred. When pushed well over the threshold, the laser's output changed from being monomodal to being multimodal. There is a possibility that a single fibre end might release more than 4 mW of power (Wang et al., 1994). [36]

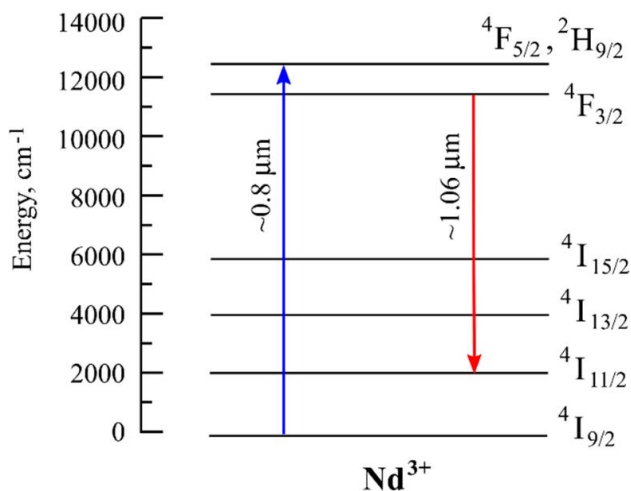


**Figure 1: A streamlined representation of the energy level diagram for  $Nd$ -doped tellurite glass. (Anashkina et al., 2020) [37]**

**Laser Amplification in  $Nd$ -Doped Microspheres:** Numerous experiments (Sasagawa et al., 2002; Sasagawa et al., 2003; Kishiet al., 2012; Kishiet al., 2015; Kumagai et al., 2015) [38-42] have shown that  $Nd$ -doped tellurite microspheres pumped by Ti:sapphire lasers are capable of lasing in the wavelength range of 1058-1075 nm. 2002 saw the debut of the very first live demonstration of a tellurite microlaser. By applying heat from a Kanthal wire heater to one end of a glass wire, it was possible to create wires with diameters ranging from fifty to several hundred millimetres. It was determined that a Ti:sapphire laser with an operating wavelength of 800 nm would be most effective for pumping microspherical resonators. The pump light of the microsphere was focussed in a location that was somewhat offset from the geometrical centre of the microsphere. The output of the 1.06-meter laser beam was captured with the help of a multimode fibre. An incidence pump threshold of 81 mW was found in a microsphere laser with a diameter of 140 m and a pump connection that was not changed.

It was shown in 2003 that quarter wavelength shifted distributed feedback resonators fabricated on the surface of microspherical samples may be used to alter the oscillation wavelengths of microlasers. This was one of the major breakthroughs in the field of microlaser research. The wavelengths that were obtained were identical to the Bragg wavelengths that were estimated using the effective refractive indices of WGMs and the grating timings that were known. Both the connections for the pump light and the collection of the output radiation were accomplished with the use of tapered optical fibres. We discovered that the threshold for a microsphere-based laser with a Q-factor of 105 was much lower than 40 milliwatts. The formation of single-mode and multimode waves was seen for spherical sizes ranging from 70 to 180 m.

Microspheres made of  $Nd$ -doped tellurite glass with air bubbles inside of them were manufactured and analysed. The method of localised laser heating was used during the production of these samples. There were periodic spectral peaks produced as a consequence of pumping the edge area of the microspherical sample, which included an air bubble with a diameter of 1.6 metres and a radius of 20 metres. These summits were designated as WGMs. However, when the location of the bubble was changed, not only WGMs but also a wide variety of other wavelengths were activated. "non-WGMs excitation" was shown to lower the threshold when it was introduced into the microresonator in the form of an air bubble. We were able to attain the lowest lasing threshold that was estimated, which was 0.034 mW for a 4-m microsphere that included an air bubble.

Azam et al., 2017: It has been shown that neodymium-doped tellurite glass is among the top options for usage in photonic applications. At a wavelength of 1.06 micrometres,  $Nd^{3+}$  ions are well

known for their effectiveness as lasing ions. On the other hand, there is a need for more discussion on the efficiency of the lasing activity of the  $\text{Nd}^{3+}$  doped tellurite glass, in particular regarding the involvement of atom-atom and atom-ligand bonding in accordance with the Judd-Ofelt hypothesis. This study has taken the initiative to evaluate the efficiency of a laser by using oscillator strength and Judd-Ofelt parameters since it is possible to utilise these factors to do so. In order to determine the optical behaviour, it is necessary to first create Nd-doped tellurite glass of an exceptional quality. The results indicate that the experimental and anticipated oscillator strengths of the glass vary from a low of  $1.157 \times 10^{-6}$  to a high of  $0.804 \times 10^{-6}$  and from a high of  $2.527 \times 10^{-6}$  to a low of  $2.243 \times 10^{-6}$ , respectively. This variation is caused by the different proportions of  $\text{Nd}_2\text{O}_3$  in the glass. The fact that the experimental and calculated oscillator strengths only differ by a minimum 10% in terms of their rms values demonstrates that there is an outstanding match between the two. In the meanwhile, it has been shown that the Judd-Ofelt intensity parameters at times  $t = 2, 4, \text{ and } 6$  vary according to the mole% of Nd that is present. Although the electric dipole makes a contribution to the  $4F_{3/2} \rightarrow 4I_{11/2}$  transition for 1.06  $\mu\text{m}$  emission in its whole, which is advantageous for lasers and optical amplification, the magnetic dipole has no effect on the process. In the following, we will go even further into discussion of a select few more discoveries. [43]

LiviuBolundut et al. 2017. Doping some lead tellurite glass ceramics with varying amounts of neodymium oxide ( $\text{Nd}_2\text{O}_3$ ) and co-doping them with fixed amounts of silver (metallic silver nanoparticles ( $\text{AgNPs}$ ), and silver oxide) allowed us to investigate the effects of this doping using photoluminescence spectroscopy (PL), diffuse reflectance ultraviolet-visible (DR-UV-vis), X-ray diffraction (XRD), density, and magnetic susceptibility. These methods made it possible for us to ( $\text{Ag}_2\text{O}$ ). After being analysed to determine whether or not they were present, the samples were analysed using a DR-UV-vis spectrometer, which indicated that the samples contained  $\text{Nd}^{3+}$  ions. It is fair to hypothesise that the couplings between  $\text{Nd}^{3+}$  and ligands have an ionic nature given the fact that the bonding value is negative for samples that have been co-doped with both  $\text{AgNPs}$  and  $\text{Ag}_2\text{O}$ . This is because the bonding value is negative for samples that have both of these dopants. The findings of the photoluminescence studies indicate that a concentration of 1 mol% of  $\text{Nd}_2\text{O}_3$  is required to quench the light given off by the substance. When the concentrations are lower than that threshold, the PL peaks are less noticeable. When the concentration of  $\text{Nd}_2\text{O}_3$  is less than 3 mol%,  $\text{Nd}^{3+}$  ions have the potential to exist as solitary species or to take part in dipole-dipole interactions. On the other hand, when the concentration of  $\text{Nd}_2\text{O}_3$  is higher, they are only capable of existing as species that are connected by antiferromagnetic interactions. [44]

The process of melt-quenching was used in order to produce a sizeable number of tellurite glasses that were enriched with neodymium nanoparticles (Azlina et al., 2020). To make the glasses, the components  $(\text{TeO}_2)_{0.7}(\text{B}_2\text{O}_3)_{0.3}(\text{ZnO})_{0.31-x}(\text{Nd}_2\text{O}_3 \text{ NPs})_x$  were employed, where  $x$  denoted 0.005, 0.01, 0.02, 0.03, 0.04, and 0.05 mol% of the overall mixture. It is possible to come across a large variety of alternative components for use in the production of glasses. After conducting the tests, we analysed the findings to determine the molar volume as well as the density of the glasses. The Z-scan method, photoluminescence, and a UV-vis spectrometer were used in this experiment in order to explore the optical characteristics of a doped tellurite glass that included nanoparticles of neodymium. In the glass network, the energy of the optical band gap is located somewhere in the range of 3.178 to 3.209 eV. Upconversion emission from the laser glass was seen in the ultraviolet region of the electromagnetic spectrum when the material was stimulated at a wavelength of 800 nanometers. Mathematical analysis and computational methodologies were used in order to ascertain the optical basicity, oxide ion polarizability, and electronic polarizability, in addition to the metallization criteria. In addition to looking at nonlinear absorption, we also looked at nonlinear refractive index and third-order susceptibilities. Tellurite and neodymium nanoparticles were combined in order to generate the laser glass that has an excellent degree of optical efficiency. [45]

Glass samples were obtained by the authors of the research by Shighihalli et al. (2013) by exposing them to melt quenching, and the findings indicated that the samples contained the following chemical compositions (in mole percent): boron, carbon, silicon, boron carbide, boron nitride, boron nitride, boron A combination that is made up of  $x$  mols of neodymium dioxide, 60 mols of boron oxide, and 20 mols each of lead oxide and tin oxide (where  $x$  may be any of the following values: 0, 1, 2, 3, or 4). After the samples had been cooled to room temperature, differential scanning calorimetry was used in order to validate the vitreous nature of the samples. The powder analysis provided support for the concept that the glasses have an amorphous structure when it comes to X-ray diffraction. Following the application of the Judd-Ofelt (JO) analysis to the UV-visible absorption spectra, the creation of JO parameters  $\Omega_\lambda$  ( $\lambda = 2, 4, \text{ and } 6$ ) was accomplished. It would seem that the ratio of two to six to four is the norm across the board. The importance of the number 2 suggests that there is an establishment of covalent bonds between the  $\text{Nd}^{3+}$  ions and the ligands that are in the vicinity. It is possible to make an estimate of each of the following: radiative lifetimes, branching ratios, and radiative transition probabilities. It is probable that these glasses will find use in lasers due to the increased branching ratio and emission-to-excited-state absorption

intensity ratio that they display throughout the  $4F_{3/2} \rightarrow 4I_{11/2}$  transition. [46]

Mohammad Reza Dousti and Raja Junaid Amjad. 2016: Improving the emission cross section of transparent oxide glasses that have been doped with rare earth (RE) ions is a difficult task. These glasses have a very low emission cross section when compared to others. The technique by which metal nanoparticles (NPs) increase emission quality is the subject of considerable disagreement; yet, this has not stopped their use as a practical approach. The optical absorption and emission characteristics of tellurite glass are now being investigated by researchers. The tellurite glass in question has been doped with  $Nd^{3+}$  ions and silver nanoparticles. At a wavelength of around 522 nm, silver nanoparticles exhibit a surface plasmon band that is visible to the naked eye.  $Nd^{3+}$  ions have the potential to get excited and absorb light in a wide variety of locations throughout the visible light spectrum. The energy levels at which the transitions between the ground state and the different excited states take place are seen in these bands, which demonstrate where those transitions take place. These bands also show where the various excited states occur. When  $AgNO_3$  is injected at concentrations of up to one mole percent, the luminescence of  $Nd^{3+}$  ions at 1.06  $\mu m$  is increased by a factor of three. This spike in luminescence can be seen very clearly. This takes place whenever the luminescence is stimulated by a laser with a wavelength of 800 nm. The hypothetical interactions that take place between RE ions and metal ions may be characterised in terms of the potential energy transfer that takes place as well as the local field enhancements that take place. [47]

Doping was performed on glass ceramics comprised of lead tellurite by adding silver ( $Ag_2O$  or  $Ag$  metallic nanoparticles,  $AgNPs$ ) at concentrations that were held constant, and erbium ions in varying proportions. This was done so that research could be conducted on the optical, spectroscopic, and structural properties of the glass ceramics. In order to accomplish this goal, a wide variety of techniques, including X-ray diffraction, photoluminescence (PL), diffuse reflectance ultraviolet-visible (DR-UV-vis), Fourier transform infrared (FTIR), and Fourier transform infrared, were used (XRD). The crystallographic phases that were present in the samples were analysed and characterised by making use of the data that was received from the XRD scans. This data included the quantitative ratio, average unit-cell characteristic, and crystallite size of the crystallographic phases. In accordance with the results of an FTIR spectroscopy investigation, the glass ceramic network seems to be mostly composed of  $TeO_3$  and  $TeO_4$  structural units. When there is an increase in the quantity of  $Er_2O_3$  present, the transformation of  $TeO_3$  into  $TeO_4$  is started, but this process is also impacted by the kind of codopant that is detected in the samples ( $Ag_2O$  or  $AgNPs$ ). We were able to discover, via the use of the DR-UV-vis spectra, that the values of the optical band gap decreased in conjunction with an increase in the

quantity of erbium that was present in the samples. In the course of the investigation, it was found that the materials that were used had  $Er^{3+}$  ions at about 525 and 547 nm, in addition to  $Pb^{2+}$  ions at approximately 430 and 708 nm. It was found that the light emission of  $Er^{3+}$  ions was adversely influenced (suppressed/increased) by the addition of  $Er^{3+}:Ag$  to the materials that were being investigated for this particular research project. This was discovered as a result of the discovery that the light emission of  $Er^{3+}$  ions was adversely influenced (suppressed/increased). [48]

## CONCLUSION

In conclusion, we found that there are significant advancements that have taken place in manufacture, design, analysis and applications of the lead based telluride glasses. Our study has comprehensively mentioned that have been carried out from last decade. Our review could help researchers across the globe in getting easy literature review for their studies on lead based telluride glasses.

## ACKNOWLEDGEMENT

We are highly thankful to the Department of Physics, Faculty of Science and IT, Madhyanchal Professional University, Ratibad, Bhopal and especially the Research Department for helping in carrying this study.

## CONFLICT OF INTEREST

None to Declare.

## REFERENCES

1. G.S. Murugan, E. Fargin, V. Rodriguez, F. Adamietz, M. Couzi, T. Buffeteau, P. LeCoustumer, Temperature-assisted electrical poling of  $TeO_2$ - $Bi_2O_3$ - $ZnO$  glasses for nonlinear optical applications, *Journal of Non-Crystalline Solids*, 344 (2004) 158-166.
2. R.F. Souza, M.A. Alencar, J.M. Hickmann, R. Kobayashi, L.R. Kassab, Femtosecond nonlinear optical properties of tellurite glasses, *Applied physics letters*, 89 (2006) 171917.
3. Y. Chen, Q. Nie, T. Xu, S. Dai, X. Wang, X. Shen, A study of nonlinear optical properties in  $Bi_2O_3$ - $WO_3$ - $TeO_2$  glasses, *Journal of Non-Crystalline Solids*, 354 (2008) 3468-3472.
4. T.T. Fernandez, S. Eaton, G. Della Valle, R.M. Vazquez, M. Irannejad, G. Jose, A. Jha, G. Cerullo, R. Osellame, P. Laporta, Femtosecond laser written optical waveguide amplifier in phospho-tellurite glass, *Optics express*, 18 (2010) 20289-20297.
5. S. Manning, A study of tellurite glasses for electro-optic optical fibre devices, Ph.D. Dissertation, University of Adelaide, Australia (2011).
6. H. Burger, U. Grunke, I. Gugov, Optical tellurite glasses for optical waveguide amplifiers and

- oscillators, and process for producing them, in Google Patents, 2003.
7. P. Nandi, G. Jose, C. Jayakrishnan, S. Debbarma, K. Chalapathi, K. Alti, A. Dharmadhikari, J. Dharmadhikari, D. Mathur, Femtosecond laser written channel waveguides in tellurite glass, *Optics express*, 14 (2006) 12145-12150.
  8. E.R. Barney, A.C. Hannon, D. Holland, N. Umetsaki, M. Tatsumisago, R.G. Orman, S. Feller, Terminal oxygens in amorphous TeO<sub>2</sub>, *The Journal of Physical Chemistry Letters*, 4(2013) 2312-2316.
  9. A. Gulenko, O. Masson, A. Berghout, D. Hamani, P. Thomas, Atomistic simulations of TeO<sub>2</sub>-based glasses: interatomic potentials and molecular dynamics, *Physical Chemistry Chemical Physics*, 16 (2014) 14150-14160.
  10. R.A. El-Mallawany, *Tellurite glasses handbook: physical properties and data*, CRC Press, 2011.
  11. R. El-Mallawany, Structural interpretations on tellurite glasses, *Materials chemistry and physics*, 63 (2000) 109-115.
  12. A. Kaur, A. Khanna, F. González, C. Pesquera, B. Chen, Structural, optical, dielectric and thermal properties of molybdenum tellurite and borotellurite glasses, *Journal of Non-Crystalline Solids*, 444 (2016) 1-10.
  13. A. Kaur, A. Khanna, H. Bhatt, M. González-Barriuso, F. González, B. Chen, M. Deo, BO and Te-O speciation in bismuth tellurite and bismuth borotellurite glasses by FTIR, 11BMAS-NMR and Raman spectroscopy, *Journal of Non-Crystalline Solids*, 470 (2017) 19-26.
  14. N. Gupta, A. Kaur, A. Khanna, F. González, C. Pesquera, R. Iordanova, B. Chen, Structure-property correlations in TiO<sub>2</sub>-Bi<sub>2</sub>O<sub>3</sub>-B<sub>2</sub>O<sub>3</sub>-TeO<sub>2</sub> glasses, *Journal of Non-Crystalline Solids*, (2017) 168-177.
  15. E. Hecht, *Optics*, Pearson Education, 2016.
  16. H. Mueller, Theory of photoelasticity in amorphous solids, *Physics*, 6 (1935) 179-184.
  17. H. Mueller, The theory of photoelasticity, *Journal of the American Ceramic Society*, 21(1938) 27-33.
  18. M. Guignard, J. Zwanziger, Zero stress-optic barium tellurite glass, *Journal of Non-Crystalline Solids*, 353 (2007) 1662-1664.
  19. T.K. Bechgaard, J.C. Mauro, L.M. Thirion, S.J. Rzoska, M. Bockowski, M.M. Smedskjaer, Photoelastic response of permanently densified oxide glasses, *Optical Materials*, 67 (2017) 155-161.
  20. M. Guignard, L. Albrecht, J. Zwanziger, Zero-stress optic glass without lead, *Chemistry of Materials*, 19 (2007) 286-290.
  21. Sayyed MI, Kumar A, Alhuthali A, Mahmoud KA, Al-Hadeethi Y. Tailoring Dy<sup>3+</sup>/Tb<sup>3+</sup>-doped lead telluride borate glasses for gamma-ray shielding applications. *The European Physical Journal Plus*. 2021 Feb;136(2):1-6.
  22. Li P, Qi X, Wang LM. A comprehensive study of lead telluride (PbTe)-based amorphous alloys: Glass formation and thermoelectric properties. *Journal of Non-Crystalline Solids*. 2021 Nov 1;571:121057.
  23. Sathish M, Eraiah B. Synthesis and structural characterization of niobium doped lead-telluride glass-ceramics. *In IOP Conference Series: Materials Science and Engineering 2015 Feb 17 (Vol. 73, No. 1, p. 012137)*. IOP Publishing.
  24. El-Rabaie S, Taha TA, Higazy AA. Characterization and growth of lead telluride quantum dots doped novel fluorogermanate glass matrix. *Materials Science in Semiconductor Processing*. 2015 Feb 1;30:631-5.
  25. Krataitong C, Srichai K, Tubtimtae A. Structural and optical properties of undoped and antimony-doped lead telluride thin films. *Materials Letters*. 2021 Feb 15;285:129085.
  26. Sathish M, Eraiah B, Anavekar RV. Preparation and Characterization of Niobium Doped Lead-Telluride Glass Ceramics. *In AIP Conference Proceedings 2011 Jul 15 (Vol. 1349, No. 1, pp. 569-570)*. American Institute of Physics.
  27. Riyatun LR, Marzuki A. Physical and optical properties of lead doped tellurite glasses. *In IOP Conf. Ser. Mater. Sci. Eng 2016 (Vol. 107)*.
  28. Saheb PZ, Asokan S, Gowda KA. Electrical switching studies of lead-doped germanium telluride glasses. *Applied Physics A*. 2003 Oct;77(5):665-8.
  29. Bomfim FA, Martinelli JR, Kassab LR, Wetter NU, Neto JJ. Effect of the ytterbium concentration on the upconversion luminescence of Yb<sup>3+</sup>/Er<sup>3+</sup> co-doped PbO-GeO<sub>2</sub>-Ga<sub>2</sub>O<sub>3</sub> glasses. *Journal of non-crystalline solids*. 2008 Nov 1;354(42-44):4755-9.
  30. Wang G, Xu S, Dai S, Yang J, Hu L, Jiang Z. Thermal stability, spectra and laser properties of Yb: lead-zinc-telluride oxide glasses. *Journal of non-crystalline solids*. 2004 May 1;336(2):102-6.
  31. Al Mohammedi W, El Damrawi G, Sherbiny M, Mohamed Abdelghany AM. Structure-properties correlation based on tellurite glasses modified by silver oxide and lead iodide. *Bulletin of Materials Science*. 2022 Jun;45(2):1-7.
  32. Urban JJ, Talapin DV, Shevchenko EV, Murray CB. Self-assembly of PbTe quantum dots into nanocrystal superlattices and glassy films. *Journal of the American Chemical Society*. 2006 Mar 15;128(10):3248-55.
  33. Silva MA, Messaddeq Y, Ribeiro SJ, Poulain M, Villain F, Briois V. Structural studies on TeO<sub>2</sub>-PbO glasses. *Journal of Physics and Chemistry of Solids*. 2001 Jun 1;62(6):1055-60.
  34. Richards, B.D.; Jha, A. Lasers utilising tellurite glass-based gain media. In *Technological Advances in Tellurite Glasses*; Rivera, V.A.G., Manzani, D., Eds.; Springer: Berlin, Germany, 2017; Volume 254, pp. 101-130. [CrossRef]
  35. Michel, J.C.; Morin, D.; Uzel, F. Propriétés spectroscopiques et laser d'un verre tellurite et d'un verre phosphate fortement dopés en néodyme. *Revue Phys. Appl.* 1978, 13, 859-866. [CrossRef]
  36. Wang, J.S.; Machewirth, D.P.; Wu, F.; Snitzer, E.; Vogel, E.M. Neodymium-doped tellurite

- single-mode fiberlaser. *Opt. Lett.* 1994, 19, 1448–1449. [CrossRef]
37. Anashkina EA. Laser sources based on rare-earth ion doped tellurite glass fibers and microspheres. *Fibers.* 2020 May 11;8(5):30.
  38. Sasagawa, K.; Kusawake, K.; Ohta, J.; Nunoshita, M. Nd-doped tellurite glass microsphere laser. *Electron. Lett.* 2002, 38, 1355–1357. [CrossRef]
  39. Sasagawa, K.; Yonezawa, Z.; Ohta, J.; Nunoshita, M. Control of microsphere lasing wavelength using 4-shifted distributed feedback resonator. *Electron. Lett.* 2003, 39, 1817–1819. [CrossRef]
  40. Kishi, T.; Kumagai, T.; Yano, T.; Shibata, S. On-chip fabrication of air-bubble-containing Nd<sup>3+</sup>-doped tellurite glass microsphere for laser emission. *AIP Adv.* 2012, 2, 042169. [CrossRef]
  41. Kishi, T.; Kumagai, T.; Shibuya, S.; Prudenzano, F.; Yano, T.; Shibata, S. Quasi-single mode laser output from a terrace structure added on a Nd<sup>3+</sup>-doped tellurite-glass microsphere prepared using localized laser heating. *Opt. Express* 2015, 23, 20629–20635. [CrossRef]
  42. Kumagai, T.; Kishi, T.; Yano, T. Low threshold lasing of bubble-containing glass microspheres by nonwhispering gallery mode excitation over a wide wavelength range. *J. Appl. Phys.* 2015, 117, 113104. [CrossRef]
  43. Azman K, Yahya N, Azhan H, Syamsyir SA, Nasuha RS. Lasing Efficiency of Nd<sup>3+</sup>-Doped Lead Tellurite Glass. In *Solid State Phenomena 2017* (Vol. 268, pp. 186-190). Trans Tech Publications Ltd.
  44. Bolundut L, Pop L, Bosca M, Tothazan N, Borodi G, Culea E, Pascuta P, Stefan R. Structural, spectroscopic and magnetic properties of Nd<sup>3+</sup>-doped lead tellurite glass ceramics containing silver. *Journal of Alloys and Compounds.* 2017 Jan 25;692:934-40.
  45. Azlina Y, Azlan MN, Halimah MK, Umar SA, El-Mallawany R, Najmi G. Optical performance of neodymium nanoparticles doped tellurite glasses. *Physica B: Condensed Matter.* 2020 Jan 15;577:411784.
  46. Shigihalli NB, Rajaramakrishna R, Anavekar RV. Optical and radiative properties of Nd<sup>3+</sup>-doped lead tellurite borate glasses. *Canadian Journal of Physics.* 2013;91(4):322-7.
  47. Dousti MR, Amjad RJ. Enhanced 1.06 μm emission in Nd<sup>3+</sup>-doped lead-tellurite glasses doped with silver nanoparticles. *Journal of Nanophotonics.* 2016 Nov;10(4):046010.
  48. Culea E, Vida-Simiti I, Borodi G, Culea EN, Stefan R, Pascuta P. Effects of Er<sup>3+</sup>: Ag codoping on structural and spectroscopic properties of lead tellurite glass ceramics. *Ceramics International.* 2014 Aug 1;40(7):11001-7.

---

#### Corresponding Author

Rajiv Pandey\*